Raman Spectra and Conformational Properties of Ribosomes during Various Stages of Disassembly†

G. J. Thomas, Jr.,* B. Prescott, and M. G. Hamilton

ABSTRACT: Raman spectra have been obtained on aqueous solutions of ribosomes, ribosomal subunits, ribosomal proteins, and ribosomal RNA extracted from both rat liver (RL) and *Escherichia coli* cells. The species examined from RL ribosomes are total ribosomes (80 S), large subunits (60 S), small subunits (40 S), EDTA-treated ribosomes, total rRNA, 28S RNA, 18S RNA, total protein, RNP particles from 80S ribosomes, and RNP particles from 60S subunits. The species examined from *E. coli* ribosomes are total ribosomes (70 S), large subunits (50 S), small subunits (30 S), mixtures of 50S and 30S subunits, total rRNA, 23S RNA, and 16S RNA. All rRNA molecules are shown by Raman spectroscopy to contain highly ordered secondary structures in which the backbone conformations are predominantly of the A-helix type. The present Raman spectra do not contain sufficient detail, however, to reach firm conclusions about the conformations of ribosomal proteins or their mutual interactions. RNA molecules within ribosomal particles remain highly ordered during various stages of ribosome disassembly, and their conformations are generally invariant to perturbations of ribosome structure, including dissociation into subunits, EDTA treatment, and partial deproteinization in a CsCl density gradient. However, when total protein extraction is carried out on ribosomes and subunits, small but significant changes in rRNA secondary structure are detected. The kind and magnitude of secondary structural change are different for different ribosomal particles. The Raman spectra of the ribosomes are compared also with spectra of a model ribonucleoprotein, the complex formed by poly(riboadenylic acid) and poly(L-arginine).

In terms of mass the ribosome is the main component of the cellular apparatus for the translation of genetic information into protein. It has a complex structure and multiple functions in protein synthesis. While the primary structure of the *Escherichia coli* ribosome is almost solved and many studies have been made of its secondary and tertiary structures (Brimacombe et al., 1976), far less is known about the structure of eukaryotic ribosomes at any level. The aim of this research was to determine details of the structure and interactions of the RNA and proteins of a representative eukaryotic ribosome, that of rat liver (RL), in specific stages of assembly and to compare the results with data obtained on the *E. coli* ribosome.

Many physical techniques have been used to study ribosome structure (Van Holde & Hill, 1974; Lake et al., 1974a,b; Stöffler & Wittmann, 1977; Serdyuk & Grenader, 1977; Cox, 1977; Damaschun et al., 1979). Early studies have shown that the RNA is not shielded by a protein shell. Rather the RNA confers structure on the particle. Spectral measurements of the hypochromism and optical anisotropy of the RNA, both free and within the particle, have shown that the secondary structure of the RNA is not greatly affected by the proteins (Cox, 1977).

The use of Raman spectroscopy in structural studies of RNA has been reviewed previously (Thomas & Kyogoku, 1977). Although recent attention has centered on tRNA and 5S RNA (Chen et al., 1978; Luoma & Marshall, 1978a,b), detailed analyses of the Raman spectra of *E. coli* rRNA have also been reported (Thomas, 1970; Thomas et al., 1971, 1973; Chen & Thomas, 1974). These studies have established a useful correlation between the spectral intensity of Raman scattering by the RNA phosphodiester group vibrations and the amount of secondary structure present in the aqueous RNA molecule (Lafleur et al., 1972; Thomas & Hartman, 1973). The Raman spectrum also provides information on the extent of hydrogen-bonded base pairing and base stacking in RNA (Thomas et al., 1971) and polyribonucleotides (Small & Peticolas, 1971).

In the case of proteins, the Raman spectrum contains information relating to the conformation of the polypeptide chain (Chen & Lord, 1974; Lippert et al., 1976; Lord, 1977), as well as to the environment of various amino acid side groups (Siamwiza et al., 1975). Recent comprehensive surveys are available (Thomas & Kyogoku, 1977; Frushour & Koenig, 1975).

In the present work Raman spectra have been obtained primarily on ribosomal particles. The spectra are complex, consisting of contributions from both RNA and protein components. However, since the Raman scattering per nucleotide residue is substantially more intense than that per amino acid residue (Thomas, 1976), the spectra of ribosome particles are dominated for the most part by Raman scattering of RNA. Where relatively intense Raman scattering from the protein does indeed occur (e.g., in the spectral regions 1200–1350 and 1500–1700 cm^{-1}, such scattering is often overlapped by comparably intense Raman scattering from the RNA. Consequently, it is difficult to measure reliably the intensities of Raman lines of protein and not feasible to monitor small intensity changes in such lines as a function of ribosome assembly. Therefore, in the discussion which follows, emphasis has been given to interpreting the Raman spectra of ribosomes and their derived particles in terms of structural features of the RNA components.

Raman spectra of high signal-to-noise ratio were obtained on RL ribosomes which were disassembled in stages proceeding from polysomes, to ribosomes, to active subunits, to protein-depleted ribonucleoproteins or "RNP particles", and finally to protein-free rRNA.

The utility of the Raman technique in nucleoprotein research has been demonstrated in previous studies of bacteriophages, plant viruses, and chromatin (Thomas, 1976). The present study represents, however, the first application of laser–Raman

† From the Department of Chemistry, Southeastern Massachusetts University, North Dartmouth, Massachusetts 02747 (G.J.T. and B.P.), and the Sloan Kettering Institute for Cancer Research, New York 10021 (M.G.H.). *Received February 1, 1980.* This work was supported by U.S. Public Health Service Grants AI 11855 and GM 24981.

0006-2960/80/0419-3604$01.00/0

spectroscopy to native ribosomes of both eukaryotic and prokaryotic origins. A preliminary discussion of these results has been given recently (Hamilton et al., 1979).

Experimental Procedures

General Procedures. Analytical grade reagents and ultrapure sucrose and guanidine hydrochloride (Gdn·HCl) were used.

For initial separations of species of all ribosome preparations, zonal centrifugations in 8–40% (w/v) sucrose gradients containing the appropriate buffer and salts were carried out in batch-type zonal rotors at 4 °C. Salt–puromycin dissociated RL ribosomes and all RNA preparations were run at 20 °C. RL ribosomes or subunits were recovered by precipitation with 0.2 volume of ethanol after adjustment of the $MgCl_2$ concentration to 10 mM (Kaulenas, 1971). For RL subunits in 0.5 M KCl and 5 mM $MgCl_2$, this was accomplished by the addition of 2 volumes of 12 mM $MgCl_2$ before ethanol precipitation in order to decrease the KCl concentration. *E. coli* ribosomes and subunits required the addition of 0.7 volume of ethanol for precipitation. RNA was precipitated by the addition of 2 volumes of ethanol. Ethanol precipitations were carried out by adding ethanol, prechilled to −20 °C, to the sample at 4 °C. The suspensions were usually stored at −20 °C overnight before centrifugation. Some samples were recycled through sucrose gradients in a Beckman SW 27 rotor.

Physical Characterization of the Samples. A Beckman Model E analytical ultracentrifuge equipped with ultraviolet absorption photoelectronic scanner optics was used to assess the monodispersity of each sample by its sedimentation velocity (Hamilton, 1974).

Preparation of Rat Liver Ribosomes, 80S Monomers, and Subunits. Total cytoplasmic ribosomes were isolated and purified from the livers of fasted adult male white rats as described by Petermann (1971). This method yields ribosomes attached to mRNA fragments as judged by their endogenous activity in in vitro protein synthesis. Further purification to remove a faint yellow color, presumed to be ferritin, was achieved by two steps of ethanol precipitation.

Runoff 80S ribosomes were isolated by zonal centrifugation after incubation for 30 min at 37 °C in a complete system for protein synthesis as described by Staehelin & Falvey (1971). After dialysis for 2 h in the cold against 30 mM KCl, 3 mM potassium phosphate, pH 7.3, 1 mM $MgCl_2$, and 1 mM dithiothreitol, the ribosomes were loaded onto the sucrose gradient containing the same solvent.

Ribosomes were dissociated into subunits essentially by the method of Blobel & Sabatini (1971). Ribosomes were dialyzed overnight in the cold against 0.5 M KCl, 20 mM Tris-HCl, pH 7.4 at 20 °C, and 5 mM $MgCl_2$. The solution was made 1 mM in puromycin by the addition of 0.1 volume of 10 mM neutralized puromycin and, after 10 min at 4 °C, the solution was incubated for 15 min at 37 °C, brought to room temperature, and loaded onto a sucrose gradient containing 0.5 M KCl, 10 mM triethanolamine hydrochloride, pH 7.4, and 5 mM $MgCl_2$. Since RL subunits cannot be frozen in 0.5 M KCl, the alcohol-precipitated subunits were resuspended in 30 mM KCl, 10 mM triethanolamine hydrochloride, pH 7.4, 1 mM $MgCl_2$, and 8% sucrose for storage at −20 °C.

Preparation of E. coli Ribosomes and Subunits. Two batches of *E. coli* ribosomes were used. The first was isolated from the ribonuclease-deficient strain BL 15, the gift of Dr. Peter Model (Rockefeller University, New York, NY). The frozen cells were lysed in a phase-transition press. The lysate was diluted with 2 volumes of 50 mM Tris-HCl, pH 7.3, 30 mM NH_4Cl, 10 mM $MgCl_2$, and 2.4 mM glutathione before treatment with DNase. The procedures of Staehelin & Maglott (1971) were followed to purify the ribosomes. The final product consisted largely of subunits, which were separated by zonal centrifugation in 0.2 M NH_4Cl, 20 mM Tris-HCl, pH 7.2, and 3 mM $MgCl_2$.

The second batch of ribosomes was the gift of Drs. Pnina Spitnik-Elson and David Elson (The Weizmann Institute, Rehovoth, Israel), who isolated and purified them (Spitnik-Elson et al., 1978). Monodisperse 70S ribosomes were isolated by zonal centrifugation in 0.2 M NH_4Cl, 10 mM Tris-HCl, pH 7.8, and 10 mM magnesium acetate. After dialysis for 1 h against 0.2 M potassium acetate, 10 mM Tris-HCl, pH 7.8, and 1 mM magnesium acetate, the dissociated subunits were separated by zonal centrifugation.

Extraction of Ribosomal RNAs. Total RNA was extracted by a modification (Pavlovec et al., 1978) of the Gdn·HCl method of Cox (1968). In each milliliter of ribosome solution, 1 g of crystalline Gdn·HCl was dissolved and the RNA was precipitated by the addition of 1 mL of ethanol. The RNA precipitate was reextracted by 4–6 M Gdn·HCl, reprecipitated by 0.5 volume of ethanol, washed several times with ethanol, and redissolved in 0.1 M NaCl, 10 mM Tris-HCl, pH 7.2, 1 mM Na_2EDTA, and 0.2% sodium dodecyl sulfate for separation of species by zonal centrifugation.

Partial Deproteinization of RL Ribosomes and RL Large Subunits. To 1.8 mL of the sample in 30 mM KCl, 4 mM potassium cacodylate, pH 7, and 1 mM $MgCl_2$, was added 3 mL of CsCl (saturated at 25 °C) for centrifugation at 40 000 rpm in a Beckman SW 50.1 rotor for 67 h at 20 °C. Material banding in turbid layers at buoyant densities from 1.60 to 1.66 g/mL was diluted with water to fill a 2-mL tube and pelleted by overnight centrifugation at 40 000 rpm.

Extraction of RL Ribosomal Protein. Ethanol-precipitated ribosomes were dissolved in 1 volume of glacial acetic acid approximately equal to twice the pellet volume. One-tenth volume of 1 M $MgCl_2$ was also added. The supernatant solution, which exhibited an ultraviolet absorption spectrum of protein, was dialyzed successively against 20, 10, and 5% acetic acid over a period of several days. The dialysis bag was then covered with dry Sephadex G-200 in order to increase the protein concentration to ~ 40 A_{280} units/mL.

Sample Preparation for Raman Spectroscopy. Samples of ribosomes or subunits were dialyzed against 30 mM KCl, and 4 mM potassium cacodylate, pH 7, containing appropriate amounts of $MgCl_2$. The solutions were clarified by low-speed centrifugation at 10000*g* before pelleting at 100000*g* in 2-mL cellulose nitrate tubes. Cores of the pellets were introduced into the Raman capillary tubes and sealed. These samples are estimated to contain $\sim 80\%$ by weight H_2O.

In the case of deuterated samples, D_2O was substituted for H_2O solvent and samples were restricted from exposure to atmospheric H_2O. The pelleted ribosomes or subunits were resuspended in buffer solutions made up in D_2O and repelleted. This step was repeated.

All protein-containing samples were stored in D_2O for up to 3 weeks prior to spectral examination to ensure deuteration of moderately slowly exchanging peptidyl NH groups.

Ribosomal RNAs were prepared in concentrated form by substituting ethanol precipitation for pelleting by centrifugation. Ethanol was removed by drying in a vacuum desiccator. Solutions of ~ 40 $\mu g/\mu L$ were prepared by dissolving the RNA in the solvent.

Raman Spectroscopy. Raman spectra were excited with the green line of wavelength 514.5 nm from a Coherent Model CR2 laser. Radiant power at the sample was ~ 300 mW.

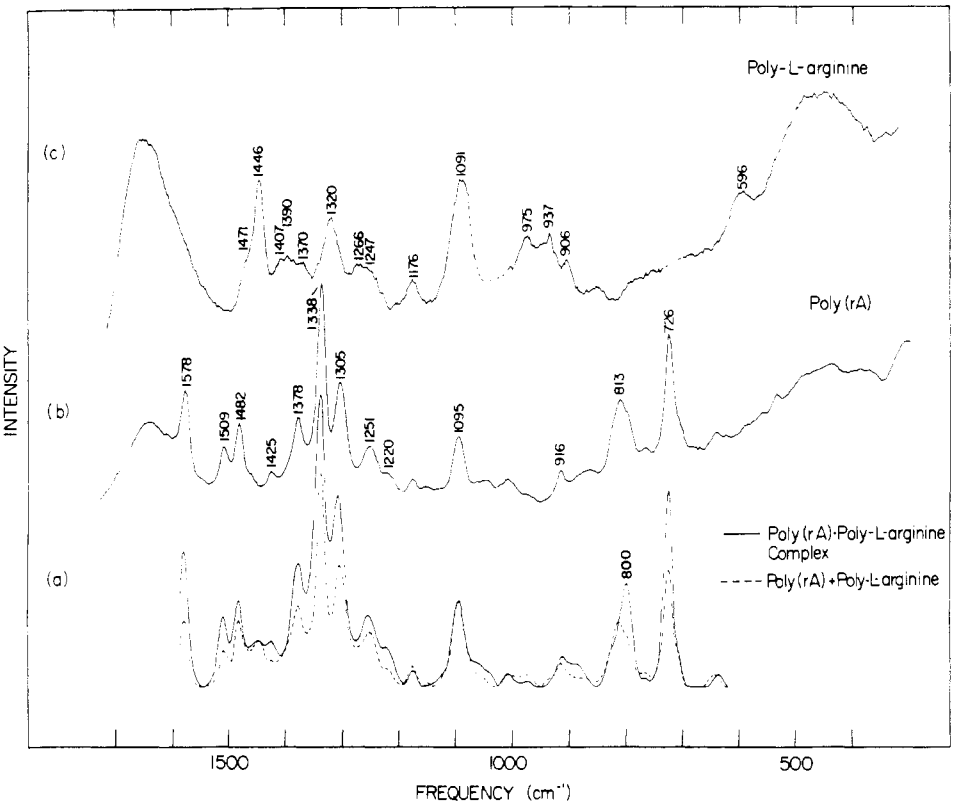

FIGURE 1: Raman spectra at 32 °C of (a) poly(rA)·poly(L-arginine) (solid suspension in 0.025 M NaCl at pH 7), (—) observed spectrum and (---) calculated spectrum from sum of constituent spectra (b + c), (b) poly(rA), 50 μg/μL in 0.025 M NaCl at pH 7, and (c) poly(L-arginine), 80 μg/μL in 0.025 M NaCl at pH 7. Instrument conditions: excitation wavelength 514.5 nm; laser power ~300 mW; spectral slit width 10 cm^{-1}; scan speed 25 cm^{-1}/min; rise time 10 s.

Spectra were recorded on a Spex Ramalog spectrophotometer. All samples were thermostated at 5 ± 1 °C, unless stated otherwise. Further details of instrumentation for Raman spectroscopy are given elsewhere (Thomas & Kyogoku, 1977). Each sample investigated was repetitively scanned. The Raman data presented and discussed represent the average of up to six scans on the given sample.

Results and Discussion

A Model Ribonucleoprotein: Poly(riboadenylic acid)·Poly(L-arginine). In order to demonstrate that significant changes can occur in the Raman spectrum accompanying moleculr interaction between model RNA and protein molecules, we present in Figure 1a the Raman spectrum of the model ribonucleoprotein poly(riboadenylic acid)·poly(L-arginine)[poly(rA)·PLA] (1:1 complex). The spectrum observed for poly(rA)·PLA is compared in Figure 1a with a sum of the spectra of poly(rA) and PLA under the same experimental conditions. It will be noted from Figure 1 that the spectrum of the complex is dominated by the Raman scattering of poly(rA).

The Raman spectrum of poly(rA) (Figure 1b) has been discussed previously in great detail (Small & Peticolas, 1971; Prescott et al., 1974). (See also the review references cited above.) The Raman spectrum of aqueous PLA (Figure 1c), though not reported previously, exhibits conformation-sensitive amide I and amide III frequencies which are similar to those of the so-called extended chain structure of poly(L-lysine) (PLL) (Prescott et al., 1976). Here, the data of Figure 1 are presented to show simply that the Raman spectrum is sensitive to interaction between poly(rA) and PLA. The major changes which occur in the Raman spectrum as a result of complex formation are interpreted as follows.

The Raman line of poly(rA) at 813 cm^{-1} which shifts to 800 cm^{-1} upon complex formation is due primarily to O–P stretching in the phosphodiester group of the ribopolymer backbone (Thomas, 1970; Thomas & Hartman, 1973). A similar shift of the phosphodiester group vibration to lower frequency occurs upon binding of PLL to poly(rA), as well as in thermal denaturation of single-stranded poly(rA) (Small & Peticolas, 1971; Prescott et al., 1974). We interpret the frequency shift as being due to a change in the configuration of the C3′–O–P–O–C5′ network in nucleotide residues of poly(rA) upon binding with polypeptide. (See also the definition of the quantity R given below.)

The prominent Raman lines of poly(rA) at approximately 726, 1305, 1338, 1378, 1509, and 1578 cm^{-1} are due to ring vibrations of adenine (Lord & Thomas, 1967). The large intensity increases which occur in these lines upon complex formation represent a loss of Raman hypochromism in poly(rA). Similar intensity increases also occur upon binding of PLL to poly(rA) (Prescott et al., 1976) and upon thermal denaturation of poly(rA) (Small & Peticolas, 1971; Prescott et al., 1974) and poly(rA)·poly(rU) (Lafleur et al., 1972).

In summary, the binding of PLA to poly(rA) perturbs the normal base-stacked secondary structure of single-stranded poly(rA) and alters the normal A-helix geometry of the poly(rA) backbone. These structural changes in poly(rA) are reflected in large intensity increases in Raman lines of the adenine ring and in a substantial shift to lower frequency of the phosphodiester group vibration.

RL Ribosomes, Subunits, and rRNA. Raman spectra of aqueous 80S ribosomes and of total rRNA and total protein extracted from 80S ribosomes are shown in Figure 2. The spectrum of 80S ribosomes is seen to be dominated by Raman scattering from its constituent rRNA. The prominent Raman

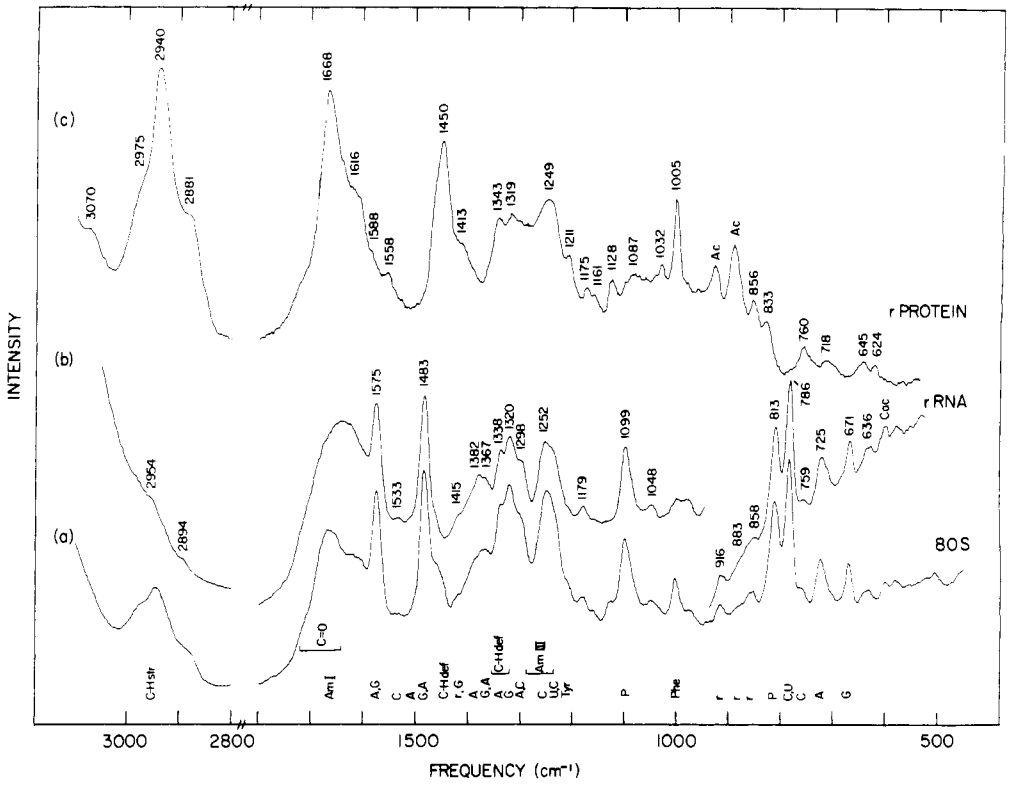

FIGURE 2: Raman spectra at 5 °C of (a) 80S ribosomes pelleted from pH 7 cacodylate buffer (0.004 M) containing 0.03 M KCl + 1.0 mM $MgCl_2$, (b) total rRNA [under same conditions as in (a)], and (c) total protein in 5% acetic acid (pH 3). Instrument conditions are the same as those in Figure 1. Similar data are obtained from D_2O solutions of 80S ribosomes and rRNA.

lines in the spectrum are assigned to residues of RNA or protein as indicated along the abscissa. Conventional abbreviations are employed for the nucleotide and amino acid residues.

The proteins isolated from 80S ribosomes are not amenable to Raman spectral analysis for reasons of low solubility at neutral pH. (This problem is not encountered when the ribosomal proteins are in combination with rRNA in the assembled ribosome.) A spectrum of satisfactory quality was obtained, however, on ribosomal protein dissolved in 5% acetic acid, as shown in Figure 2. Although the acidic solution is probably not representative of the state of the protein in 80S ribosomes, the spectrum clearly reveals the presence of specific amino acid residues: for example, phenylalanine (1005 cm^{-1}) and tyrosine (833 and 856 cm^{-1}). Amide I (1668 cm^{-1}) and amide III (1249 cm^{-1}) frequencies are prominent and suggest little α-helix and β-sheet regions in the protein chains in this solvent. We next consider the contribution of RNA to the Raman spectrum of 80S ribosomes.

An important indicator of RNA secondary structure is the ratio of intensities of Raman lines at approximately 813 and 1100 cm^{-1} ($I_{813}/I_{1100} \equiv R$). The 813-$cm^{-1}$ line of RNA, like the 813-cm^{-1} line of poly(rA), is due mainly to the symmetric O–P stretching vibration of the phosphodiester group and is sensitive to the degree of order in the RNA backbone, while the 1100-cm^{-1} line (PO_2^- symmetric stretching vibration) serves as an internal intensity standard. In solutions of nucleic acids of polynucleotides, R takes on values ranging from 0 to 1.64, depending upon the percentage of nucleotide residues which exist in regions of ordered secondary structure of the A type, including both base-paired and base-stacked regions (Lafleur et al., 1972; Thomas & Hartman, 1973). Therefore, a value of $R = 1.5$ is an indication that ~90% of the bases of rRNA are ordered under the conditions of these experiments. In Table I we have listed each of the RNA species

Table I: Percentages of Ordered Structures in rRNA Determined by Raman Intensity Measurements

state of sample	no. of spectral scans	$R \equiv I_{813}/I_{1100}$ (av)	percent order $(R/1.64)^a$
RL 80S ribosome	9	1.45 ± 0.06	88 ± 4
RL 60S subunit	4	1.47 ± 0.04	90 ± 2
RL 40S subunit	6	1.37 ± 0.02	83 ± 1
28S RNA	4	1.47 ± 0.03	90 ± 2
18S RNA	4	1.46 ± 0.05	89 ± 3
E. coli 70S ribosome	4	1.55 ± 0.06	94 ± 4
E. coli 50S subunit	4	1.58 ± 0.05	96 ± 3
E. coli 30S subunit	5	1.49 ± 0.06	91 ± 3
23S RNA	4	1.55 ± 0.09	94 ± 5
16S RNA	5	1.46 ± 0.08	89 ± 5

[a] Refer to Thomas & Hartman (1973) for details.

examined in this study along with the value of R measured from the Raman spectrum and the corresponding degree of order in RNA by using the correlation of Thomas & Hartman (1973). It will be noted that these results are entirely consistent with previously published results on *E. coli* rRNA and various tRNA species (Thomas et al., 1973; Chen et al., 1978; Luoma & Marshall, 1978a,b). It should also be kept in mind that for the purpose of calculating the percentage of order in RNA (Table I, column 4), the denominator of 1.64 is valid only when solutions of low ionic strength are considered. For solutions containing higher concentrations of Mg^{2+} or K^+ there is evidence to indicate that a normalization factor greater than 1.64 is appropriate (Thomas & Hartman, 1973; Chen et al., 1978).

Figure 2 shows that the overall secondary structure of RNA as measured by the quantity R does not change dramatically with extraction of RNA from 80S ribosomes. The absence of a frequency shift or intensity change in the 813-cm^{-1} line

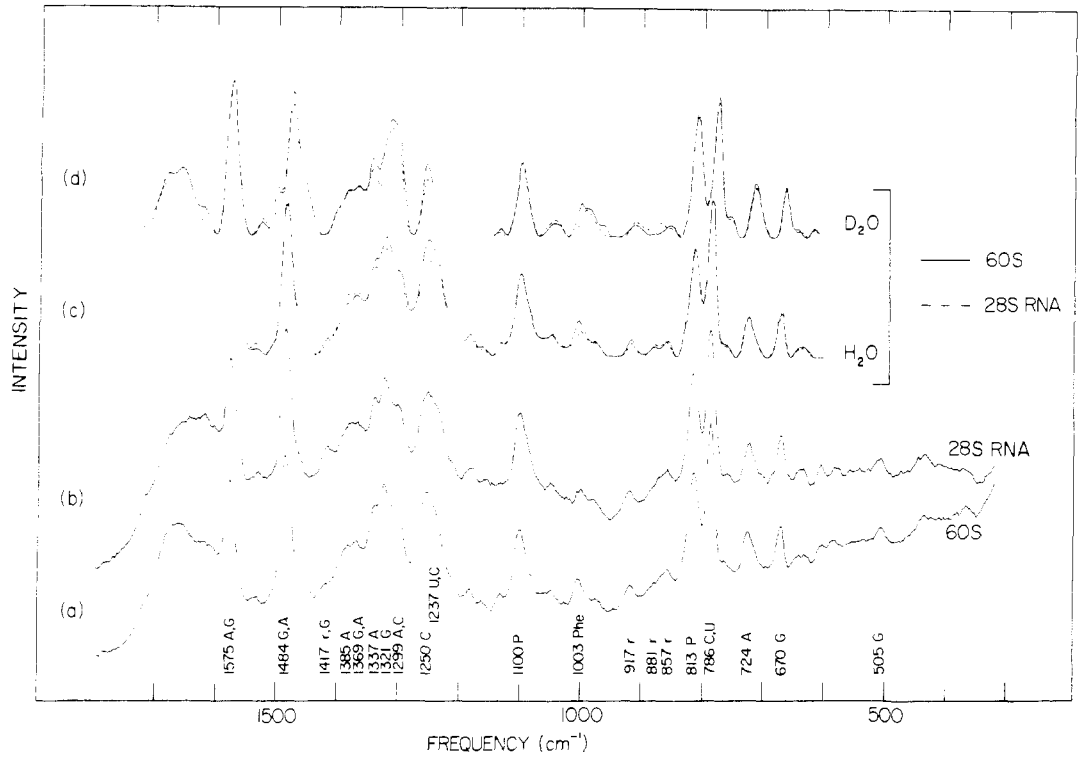

FIGURE 3: Raman spectra at 5 °C of (a) 60S subunits pelleted from pH 7 cacodylate buffer (0.004 M) containing 0.03 M KCl + 0.5 mM $MgCl_2$ and (b) 28S RNA [under same conditions as in (a)]. In (c) spectra a and b are retraced over a common base line with intensities normalized to the 1100-cm^{-1} line. In (d) corresponding spectra of D_2O solutions are retraced and normalized. Instrument conditions are the same as those in Figure 1.

and the absence of significant intensity changes in Raman lines of the RNA bases demonstrate clearly that the kind of molecular interaction which occurs between poly(rA) and PLA does not exist between RNA and proteins of 80S ribosomes. Nevertheless, the Raman spectrum of RNA within the 80S ribosome is not identical with the spectrum of RNA in the protein-free state. Relatively large intensity changes occur in the weak lines of RNA at 883 and 1415 cm^{-1}. We have assigned the former to the ribose residue (Lafleur et al., 1972) and the latter to both ribose and RNA bases (Thomas, 1970). The observed intensity changes imply an alteration of RNA structure which we shall discuss below in connection with 40S subunits.

Raman spectra of 60S subunits and 28S RNA are shown in Figure 3. The spectra are retraced over a common base line to show again that the prominent Raman lines of 28S RNA are not greatly altered by the extraction of the RNA from 60S subunits. This is true for both H_2O and D_2O solutions. Where the Raman line intensities of 60S subunits significantly exceed those of protein-free 28S RNA (ca. 1003, 1450, 1200–1350, and 1600–1700 cm^{-1}), the discrepancies can be attributed to overlapping Raman lines of the ribosomal protein. In the case of 60S subunits, there is no evidence from Raman spectra that RNA structure is altered by extraction from 60S subunits.

Raman spectra of 40S subunits and 18S RNA are shown in Figure 4. In 40S subunits, the protein contributes 57% of the total subunit mass, which is substantially greater than the percentage of protein in either 60S (36%) or 80S (52%) particles (Wool, 1979). Therefore, not unexpectedly, the spectrum of 40S subunits differs rather more markedly from that of its isolated RNA in the regions of relatively intense protein lines (ca. 1003, 1450, 1200–1300, and 1600–1700 cm^{-1}). In addition, we observe significant intensity increases in Raman lines of the bases when 18S RNA is extracted from the 40S subunit. These are as follows (Figure 4). For H_2O solutions, Raman lines of the RNA bases at 1368 (G and A), 1385 (A), 1482 (G and A), and 1506 cm^{-1} (A) increase in intensity when 18S RNA is extracted from 40S subunits. For D_2O solutions, intensity increases occur in the lines at 1367 (G and A), 1385 (A), and 1500 cm^{-1} (A). The intensity increases are substantial (10–50%) and reproducible. By analogy with model compounds (Thomas & Kyogoku, 1977), they represent a loss of Raman hypochromism due to diminished base stacking of purines upon extraction of RNA from 40S subunits.

Figure 4 also shows a small intensity change at 812 cm^{-1} as well as very large relative intensity changes in weak Raman lines of RNA groups at 882 and 1417 cm^{-1} (or 872 and 1412 cm^{-1} for D_2O solutions). These are difficult to interpret but do suggest that the conformation of the 18S RNA backbone has been altered in some fashion with extraction from 40S subunits. This effect is also observed with total RNA extraction from 80S ribosomes as stated above (see also Figure 2).

In Figure 5 we show that the Raman spectrum observed for the whole RL ribosome (80 S) is represented, to a good approximation, by the sum of the spectra of the subunits (60 S + 40 S). The 1100-cm^{-1} line is again used as the basis for normalization. The only significant and reproducible difference between the observed and computed spectra occurs in the line at 1575 cm^{-1} (G and A), which is more intense in 80S ribosomes than in 60S + 40S subunits. We believe this effect is due most probably to interference from the solvent. The absence of additional spectral differences is evidence that RNA structure is unperturbed by dissociation of 80S ribosomes into 60S and 40S subunits.

Solvent Perturbations of RL Ribosomes. Changes in actual or effective Mg^{2+} concentration are known to alter the structure and association of ribosomal subunits (Cox & Hirst,

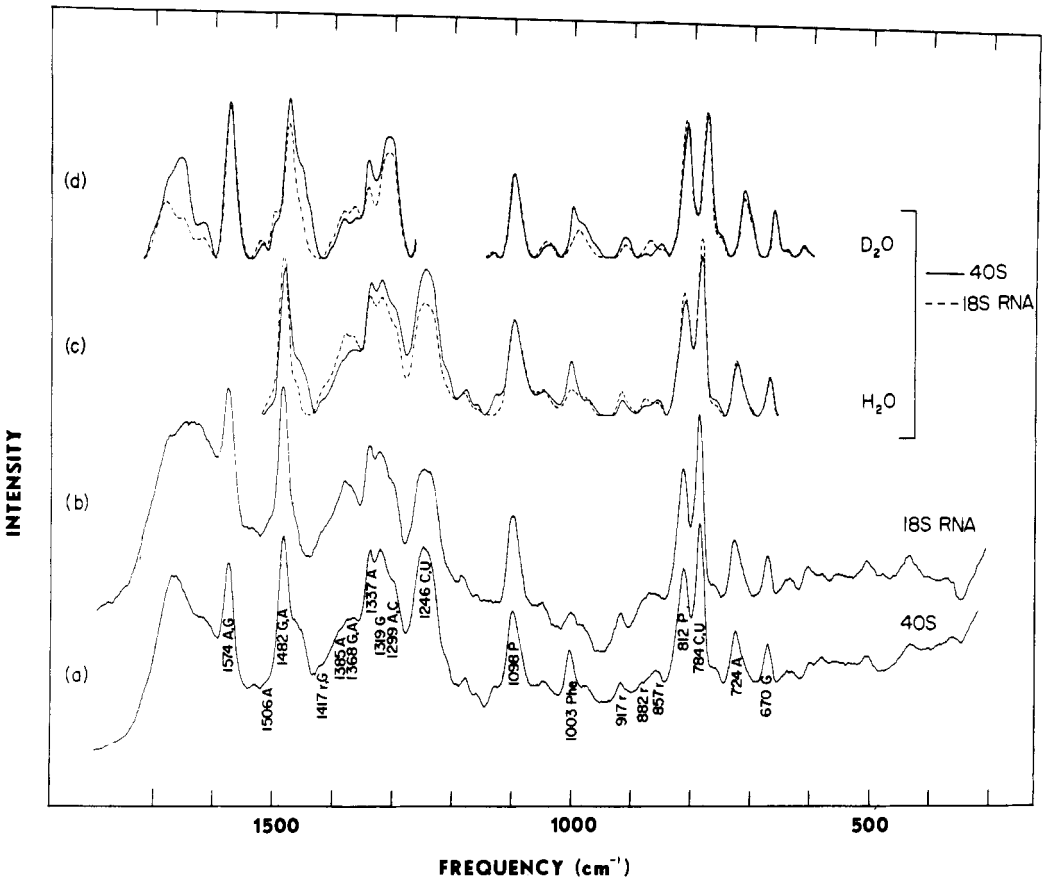

FIGURE 4: Raman spectra at 5 °C of (a) 40S subunits pelleted from pH 7 cacodylate buffer (0.004 M) containing 0.03 M KCl + 0.5 mM $MgCl_2$ and (b) 18S RNA [under same conditions as in (a)]. In (c) the spectra a and b are redrawn as in Figure 3c. In (d) the corresponding spectra of D_2O solutions are redrawn as in Figure 3d. Instrument conditions are the same as those in Figure 1.

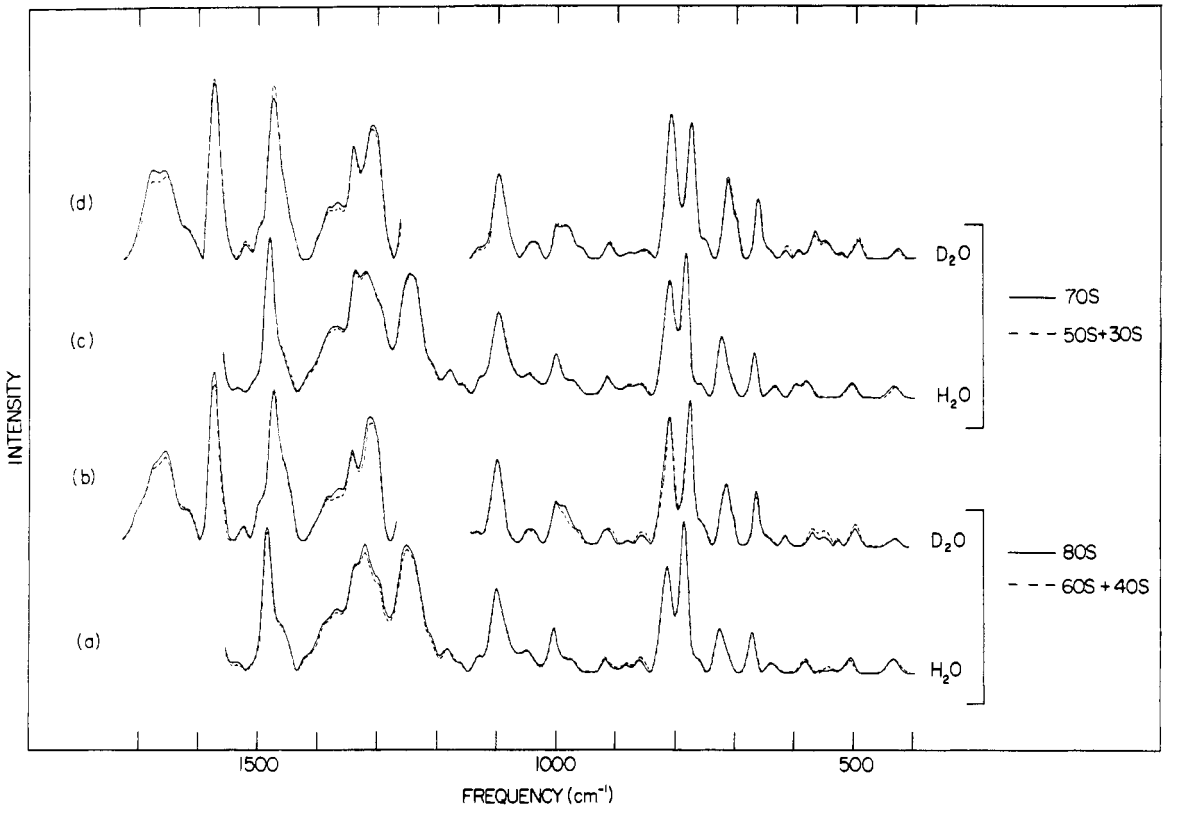

FIGURE 5: Comparison of the Raman spectrum of whole ribosomes with the sum of the spectra of subunits. (a) RL 80S ribosomes (—) and subunits (- - -) in H_2O; (b) RL 80S ribosomes (—) and subunits (- - -) in D_2O; (c) *E. coli* 70S ribosomes (—) and subunits (- - -) in H_2O; (d) *E. coli* 70S ribosomes (—) and subunits (- - -) in D_2O. All spectra are taken from Figures 2–4 and Figures 6 and 7.

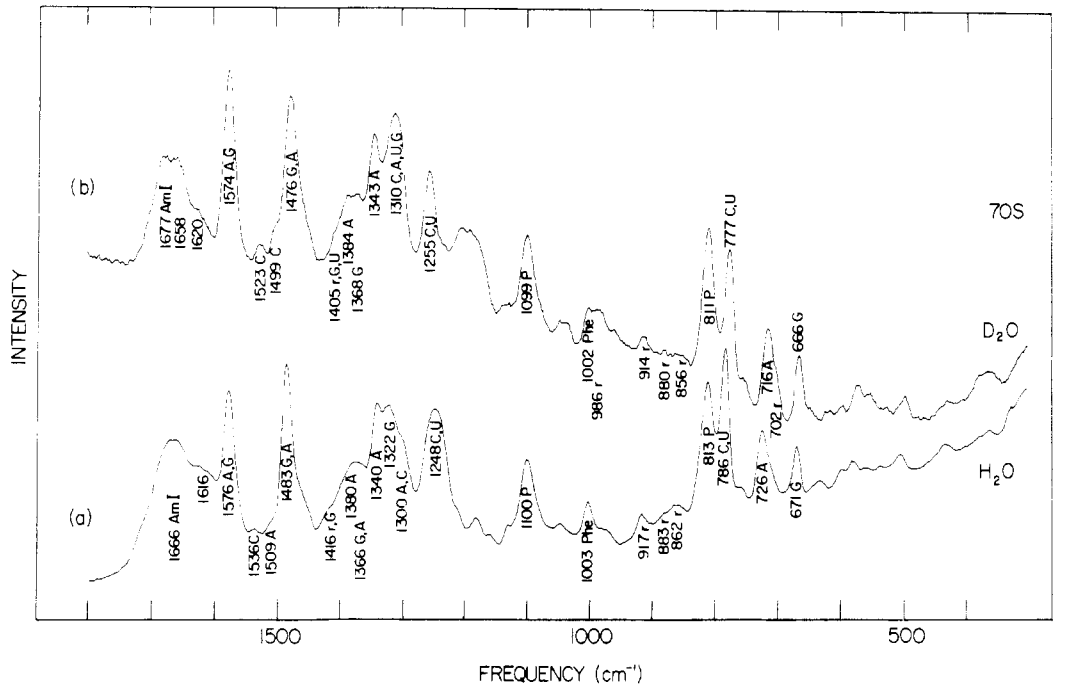

FIGURE 6: Raman spectra at 5 °C of *E. coli* 70S ribosomes pelleted from pH 7 cacodylate buffer (0.004 M) containing 0.03 M KCl and either 1 mM $MgCl_2$ (a) or 10 mM $MgCl_2$ (b). (a) H_2O solutions; (b) D_2O solutions. Instrument conditions are the same as those in Figure 1.

1976; Herbeck & Zundel, 1976; Page et al., 1967; Miall & Walker, 1969). Mg^{2+} is believed to exert its effect by stabilizing the RNA secondary structure through electrostatic screening of negatively charged phosphate groups of the RNA chain. The solutions and suspensions examined above (Figures 2–4) all contain 0.5–1.0 mM $MgCl_2$, which is considered the appropriate concentration range to stabilize ribosome structures. As Table I indicates, all rRNAs under these conditions have a highly ordered secondary structure. Moreover, we find no significant increase in the amount of ordered structure in any rRNA listed in Table I upon increasing the above-cited concentration of Mg^{2+} to 10 mM.

On the other hand, a decrease of the Mg^{2+} concentration in certain cases is expected to decrease the degree of order in rRNA. Previous studies have shown that depletion of the effective Mg^{2+} concentration through treatment with EDTA causes "unfolding" and "inactivation" or ribosomes (Page et al., 1967; Miall & Walker, 1969). Elimination of Mg^{2+} has also been shown to decrease the amount of order in tRNA (Thomas et al., 1973; Chen et al., 1975, 1978) and 5.8S RNA (Luoma & Marshall, 1978b) as monitored by Raman spectroscopy. We have therefore made Raman studies of RL ribosomes as next described.

First, we examined the Raman spectrum of RL polysomes in 0.5 M KCl, and 5 mM $MgCl_2$, conditions which yield the dissociated though active "salt subunits". The spectrum is indistinguishable from that of polysomes in 0.03 M KCl, and 1 mM $MgCl_2$ (not shown) and nearly identical with the spectrum of 80S shown in Figure 2. Thus, by the criterion of Raman spectroscopy there is no detectable change in the structure of RNA accompanying the dissociation of polysomes into the salt subunits.

Second, we isolated the 60S and 40S subunits in 0.5 M KCl, and 5 mM $MgCl_2$ and obtained the spectrum of each in that solvent as well as in 0.03 M KCl and 0.5 mM $MgCl_2$. The Raman spectrum of each subunit was found to be the same in both solvents (Figures 3a and 4a). Thus, the decreases in KCl and $MgCl_2$ concentrations also have no structural effects apparent in Raman spectra of the RNA molecules of the respective isolated subunits. Moreover, dimerization of the small subunit that occurs when the KCl concentration is reduced has no effect on the spectrum.

Third, we treated polysomes with EDTA, a procedure which should lead to partial unfolding of the subunits, loss of both 5S RNA and one protein molecule from the 60S subunit, and loss of bound tRNA and 20% of the proteins from the 40S subunit. In the course of this unfolding process, the 60S subunit is converted to a 50S particle and the 40S subunit to a 30S particle (Hamilton et al., 1971). Again, the Raman spectra of normal polysomes and unfolded 50S + 30S subunits (not shown) are indistinguishable, suggesting no significant change in overall secondary structure of rRNA accompanying the unfolding transition. Very small differences observed between the spectra can be attributed to the loss of protein molecules.

Finally, ribosomes and 60S subunits were treated with CsCl to eliminate ~50 and ~35%, respectively, of their ribosomal protein as estimated from their buoyant densities (Hamilton, 1971). Raman spectra were obtained on the resulting RNP particles. The spectra (not shown) clearly reveal the loss of protein by the diminished Raman intensity in the regions of amide III (1200–1350 cm^{-1}), CH deformations (1450–1460 cm^{-1}), aliphatic CH stretching (2800–3000 cm^{-1}), and aromatic residues (1003 cm^{-1}). Nevertheless, the Raman scattering by rRNA in RNP particles is identical with that of rRNA in the native ribosomes or subunits. Again, therefore, we find no significant change in rRNA secondary structure with partial disassembly of polysomes and 60S particles through treatment with 5 M CsCl.

E. coli. Ribosomes, Subunits, and rRNA. Figure 6 shows Raman spectra of *E. coli* 70S ribosomes in both H_2O and D_2O solutions. (See also parts c and d of Figure 5.) The *E. coli* 70S particle yields a spectrum which differs markedly from that of the RL 80S particle (cf. Figure 2) for the following reasons. First, the 70S ribosome contains much more RNA by weight than does the 80S ribosome (~70 vs. ~50%). Consequently, the Raman lines of RNA are even more dominant in the spectrum of 70S ribosomes than those in the

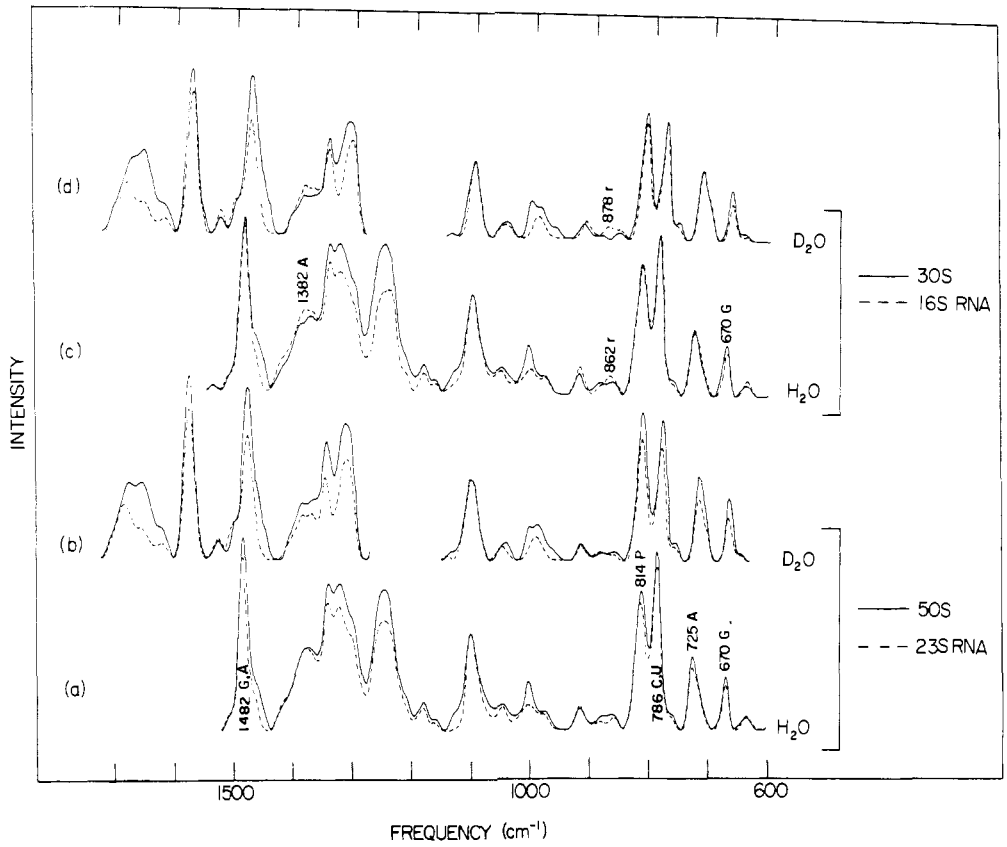

FIGURE 7: Raman spectra at 5 °C of *E. coli* subunits and RNA in H_2O and D_2O solutions. Spectra are redrawn and normalized as in Figure 3c. Each solution contains 0.004 M cacodylate buffer pH 7, 0.03 M KCl, and a minimum of 1 mM $MgCl_2$.

spectrum of 80S ribosomes. Second, *E. coli* rRNA contains proportionally more adenine than RL rRNA (25 vs. 18%). Thus, for example, the Raman line of adenine at 726 cm^{-1} (or 716 cm^{-1} for D_2O solutions) is considerably more intense for 70S ribosomes than for 80S ribosomes.

Apart from differences in primary structure, Figures 2 and 6 also reveal a significant difference in the secondary structure of rRNA in the two types of ribosomes. The Raman intensity ratio R (defined above) is consistently higher for *E. coli* rRNA than for RL rRNA. Values of R computed from the spectra are listed in Table I.

It will be noted that the values of R for 16S and 23S RNA in Table I are slightly higher than those reported previously (Thomas & Hartman, 1973; Chen & Thomas, 1974). Two factors which could account for this are the presence of 3.0 mM $MgCl_2$ and the lower solution temperature (5 °C) employed in this study.

Raman spectra of the 50S subunit and 23S RNA in H_2O and D_2O solutions are shown in Figure 7. For H_2O solutions Raman lines at 670 (G), 725 (A), 786 (C and U), 814 (OPO), and 1482 cm^{-1} (G and A) all decrease in intensity with extraction of RNA from 50S subunits. Similar intensity changes also occur for D_2O solutions. These and other lesser intensity decreases in Figure 7 cannot be accounted for simply by subtraction of the Raman scattering due to protein. Instead they indicate an overall increase in the base-stacked structure in 23S RNA upon extraction from 50S subunits. With the exception of the guanine ring mode at 670 cm^{-1}, which is hyperchromic (Thomas et al., 1971), the Raman lines in question are hypochromic and thus indicate *increased base stacking* of A, C, and U residues of 23S RNA with extraction from 50S subunits. The data indicate that the G residues of RNA are probably more stacked within the 50S subunit than in the protein-free state.

Figure 7 also shows the corresponding Raman spectra obtained on 30S subunits and 16S RNA. Extraction of RNA from 30S subunits causes the Raman lines of RNA at 862 (ribose), 1368 (A and G), and 1382 cm^{-1} (A, U, and G), among others, to increase in intensity, while the line at 670 cm^{-1} (G) again decreases in intensity. Here the data indicate *reduced base stacking* with extraction of RNA from 30S subunits.

We find that extraction of total RNA from the assembled 70S ribosome produces changes in the Raman spectrum (not shown) which are, within experimental uncertainty, the sum of changes accompanying the extractions from 30S and 50S subunits. In addition to a relatively large intensity change at 879 cm^{-1} (ribose), similar to that observed for 80S ribosomes, a net decrease occurs in the intensity of the 670-cm^{-1} line but few other large intensity changes of Raman lines due to RNA bases occur.

Finally, Figure 5 compares the observed Raman spectrum of 70S ribosomes with the sum of the spectra of dissociated 30S and 50S subunits. For both H_2O and D_2O solutions, there are no major differences between observed and summation spectra, thus indicating little if any conformational changes in RNA accompanying the dissociation of 70S ribosomes into subunits. These results are similar to those obtained on RL 80S ribosomes.

The foregoing discussions indicate that in each ribosomal subunit examined (60S and 40S particles of RL and 50S and 30S particles of *E. coli*) the RNA structure is affected differently by extraction of protein. The spectroscopic results are summarized in Table II.

Conclusions

The diagram in Figure 8 depicts the changes in state of RL ribosomes which we have investigated by Raman spectroscopy.

Table II: Raman Line Intensity Changes Accompanying Extraction of rRNA from Ribosomal Particles[a]

RL particles[b]		*E. coli* particles			assignments
80S	40S	70S	50S	30S	
		671 (−9)	670 (−16)	670 (−17)	G
		726 (−8)	725 (−16)		A
			786 (−9)		C, U
	812 (+7)		814 (−9)		P
				862 (+21)	r
883 (+33)	882 (+79)	883 (+109)			r
	1368 (+20)				G, A
	1385 (+50)			1382 (+19)	A
1415 (+62)	1417 (+87)				r
	1482 (+7)	1483 (−8)	1482 (−10)		G, A
	1506 (+111)				A

[a] Data for H_2O solutions, Figures 2-7. Raman frequencies are in cm^{-1}. Each intensity change in parentheses is the percentage increase (+) or decrease (−) in peak height. Abbreviations used: A, adenine; C, cytosine; G, guanine; U, uracil; r, ribose; P, phosphate group. [b] No significant intensity changes are detected for 60S particles.

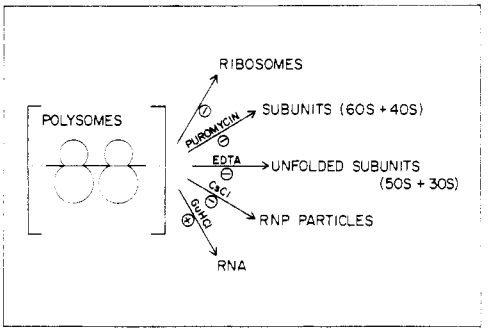

FIGURE 8: Changes in state of RL ribosomes investigated by Raman spectroscopy. The symbol ⊕ or ⊖ is used with each transition to indicate respectively whether any spectral change is observed or not observed with the transition.

We find no evidence of substantial change in RNA secondary structure when RL ribosomes or polysomes are dissociated into subunits, partially unfolded through EDTA treatment, or converted to RNP particles. Significant changes in RNA secondary structure are detected, however, when *all* of the associated ribosomal proteins are stripped from either the 80S ribosome or its 40S subunit.

These results show that the average secondary structure of RNA in RL ribosomes and subunits is independent of the state of aggregation of the subunits and independent of their partial deproteinization. On the other hand, *RL rRNA secondary structure is clearly altered by total extraction of ribosomal protein.*

In the case of *E. coli* ribosomes, the Raman spectra demonstrate that RNA secondary structure is invariant to dissociation of the ribosome into subunits. Again, however, the Raman spectra reveal significant changes in RNA secondary structure when all of the associated ribosomal proteins are stripped from the 70S ribosome. The same is true for both 50S and 30S subunits. We conclude that *E. coli rRNA secondary structure is also altered by total extraction of ribosomal protein.*

The fact that rRNA structure is altered by total protein extraction constitutes evidence for RNA–protein interactions within the ribosome. It is clear, however, that such interactions between ribosomal proteins and rRNA are not similar to the kind of peptide–nucleotide interactions occurring in poly(rA)·PLA [or in poly(rA)·PLL] complexes. In no case examined do we find the position of the conformation-sensitive 813-cm^{-1} line of rRNA shifted as a result of either association or dissociation of RNA with ribosomal protein. Hence the A-helix backbone conformation of rRNA is conserved with RNA extraction from the ribosome. Perturbations of RNA structure attendant with the removal of ribosomal proteins are apparently confined to changes in the extent of base-stacked secondary structure.

The present findings are consistent with models of ribosome structure in which a complement of tightly bound protein molecules plays a role in determining the RNA conformation. We have noted (Experimental Procedures) that chain scissions in RNA, though not extensive, are present in all ribosome preparations studied. However, it is unlikely that the secondary structural changes referred to above are the direct consequence of fragmentation of rRNA. If this were the case, secondary structural changes would probably be qualitatively similar for each subunit RNA and would also have accompanied other changes in the ribosome state depicted in Figure 8.

We note that an RNase-free strain of *E. coli* and RNase-inactivated RL ribosomes were used in this work. Hence, few scissions in RNA chains are expected to occur. The present study assumes that whatever chain scissions do occur take place at exposed locations that are not tightly bound by or to ribosomal proteins. If we assume that each rRNA species examined (28, 18, 23, or 16 S) is likely to have suffered roughly the same small degree of chain scission and roughly the same amount of fortuitous base-pairing or -stacking interactions when extracted from its respective subunit, then the data of Table II may be given a semiquantitative interpretation as follows. We consider each of the extracted aqueous RNA species to be in the same standard "reference state" and we consider the transfer of the RNA from this reference state into its corresponding native ribosomal subunit. With such a transfer, each RNA would then undergo the reverse of the Raman line intensity changes shown in Table II. We may then conclude that (1) the structure of 28S RNA is unchanged by incorporation into 60S subunits, (2) adenine residues of 18S RNA become more stacked upon incorporation into 40S subunits, (3) adenine, cytosine, and uracil residues become less stacked and guanine residues more stacked upon incorporation of 23S RNA into 50S subunits, and (4)adenine and guanine residues of 16S RNA become more stacked upon incorporation into 30S subunits.

With reference to the data of Table I, several additional conclusions can be made regarding the ordered structure of RNA. In both prokaryotic and eukaryotic ribosomes the rRNA molecules are very highly ordered (at 5 °C) with regard to the percentage of nucleotide residues that exist in regions of A-type helical geometry (Arnott, 1976). Although isolation of rRNA from the ribosome is generally accompanied by a reduction in base-stacked secondary structure (Table II), the A-helix geometry of the backbone is not greatly affected. Table I also shows that rRNA of *E. coli* is on average more ordered than rRNA of RL ribosomes. The data of Table I, when compared with the results obtained by Luoma &

Marshall (1978a,b), show that the percentages of ordered structure in 18S and 28S RNA of RL ribosomes and in 16S and 23S RNA of *E. coli* ribosomes are comparable respectively to those of 5.8S and 5S RNA in 10 mM $MgCl_2$ solutions. We have not investigated the Raman spectra of Mg^{2+}-depleted solutions of rRNA. We would expect, however, a noticeable reduction in ordered structure with depletion of Mg^{2+} as observed for tRNA (Chen et al., 1975) and 5.8S RNA (Luoma & Marshall, 1978b).

In principle, the intensities of Raman lines of rRNA in the double-bond region (1600–1700 cm^{-1}) of D_2O solutions contain information on the extent of hydrogen-bonded base pairing in RNA (Lafleur et al., 1972; Chen & Thomas, 1974). In the case of ribosomes, however, partial deuterium exchange of the ribosomal proteins complicates the interpretation and prevents any straightforward conclusions from being drawn from such data (Figure 5).

Finally, we note that the weak Raman line of RNA near 880 cm^{-1}, which has been assigned to the ribose group of RNA, is extremely sensitive to protein extractions. We are pursuing studies of model compounds to provide a basis for interpreting the apparent sensitivity of this line to RNA–protein interactions.

Acknowledgments

We thank Amalia Pavlovec and Patricia Puma for assistance in the preparation of ribosomes and Benjamin C. Gifford of the B. C. Gifford Co., Inc., for assistance in transporting ribosome samples between Sloan Kettering Institute and Southeastern Massachusetts University.

References

Arnott, S. (1976) *Life Sci. Res. Rep. 4.*

Blobel, G., & Sabatini, D. (1971) *Proc. Natl. Acad. Sci. U.S.A. 68*, 390–394.

Brimacombe, R., Nierhaus, K. H., Garrett, R. A., & Wittmann, H. G. (1976) *Prog. Nucleic Acid Res. Mol. Biol. 18*, 1–44.

Chen, M. C., & Lord, R. C. (1974) *J. Am. Chem. Soc. 96*, 4750–4752.

Chen, M. C., & Thomas, G. J., Jr. (1974) *Biopolymers 13*, 615–626.

Chen, M. C., Giege, R., Lord, R. C., & Rich, A. (1975) *Biochemistry 14*, 4385–4390.

Chen, M. C., Giege, R., Lord, R. C., & Rich, A. (1978) *Biochemistry 17*, 3134–3138.

Cox, R. A. (1968) *Methods Enzymol. 12B*, 120–129.

Cox, R. A. (1977) *Prog. Biophys. Mol. Biol. 32*, 193–231.

Cox, R. A., & Hirst, W. (1976) *Biochem. J. 160*, 505–519.

Damaschun, G., Müller, J. J., & Bielka, H. (1979) *Methods Enzymol. 59G*, 706–775.

Frushour, B. G., & Koenig, J. L. (1975) *Adv. Infrared Raman Spectrosc. 2.*

Hamilton, M. G. (1971) *Methods Enzymol. 20C*, 512–521.

Hamilton, M. G. (1974) *Methods Enzymol. 30F*, 387–395.

Hamilton, M. G., Pavlovec, A., & Petermann, M. L. (1971) *Biochemistry 10*, 3424–3427.

Hamilton, M. G., Prescott, B., & Thomas, G. J., Jr. (1979) *Proc. Int. Cong. Biochem., 11th*, 86.

Herbeck, R., & Zundel, G. (1976) *Biochim. Biophys. Acta 418*, 52–62.

Kaulenas, M. S. (1971) *Anal. Biochem. 41*, 126–131.

Lafleur, L., Rice, J., & Thomas, G. J., Jr. (1972) *Biopolymers 11*, 2423–2437.

Lake, J. A., Sabatini, D. D., & Nomura, Y. (1974a) *Ribosomes* [*Meet.*].

Lake, J. A., Pendergast, M., Kahan, L., & Nomura, M. (1974b) *Proc. Natl. Acad. Sci. U.S.A. 71*, 4688–4692.

Lippert, J. D., Tyminski, D., & Desmeules, P. J. (1976) *J. Am. Chem. Soc. 98*, 7075–7080.

Lord, R. C. (1977) *Appl. Spectrosc. 31*, 187–194.

Lord, R. C., & Thomas, G. J., Jr. (1967) *Spectrochim. Acta, Part A 23A*, 2551–2591.

Luoma, G. A., & Marshall, A. G. (1978a) *J. Mol. Biol. 125*, 95–105.

Luoma, G. A., & Marshall, A. G. (1978b) *Proc. Natl. Acad. Sci. U.S.A. 75*, 4901–4905.

Miall, S. H., & Walker, I. O. (1969) *Biochim. Biophys. Acta 174*, 551–560.

Page, L. A., Englander, S. W., & Simpson, M. V. (1967) *Biochemistry 6*, 968–977.

Pavlovec, A., Evenson, D. P., & Hamilton, M. G. (1978) *J. Gen. Virol. 40*, 239–243.

Petermann, M. L. (1971) *Methods Enzymol. 20C*, 429–433.

Prescott, B., Gamache, R., Livramento, J., & Thomas, G. J., Jr. (1974) *Biopolymers 13*, 1821–1845.

Prescott, B., Chou, C. H., & Thomas, G. J., Jr. (1976) *J. Phys. Chem. 80*, 1164–1171.

Serdyuk, I. N., & Grenader, A. K. (1977) *Eur. J. Biochem. 79*, 495–504.

Siamwiza, M. N., Lord, R. C., Chen, M. C., Takamatsu, T., Harada, I., Matsuura, H., & Shimanouchi, T. (1975) *Biochemistry 14*, 4870–4876.

Small, E. W., & Peticolas, W. L. (1971) *Biopolymers 10*, 1377–1416.

Spitnik-Elson, P., Elson, D., Abramowitz, R., & Avital, S. (1978) *Biochim. Biophys. Acta 521*, 308–323.

Staehelin, T., & Falvey, A. K. (1971) *Methods Enzymol. 20C*, 433–446.

Staehelin, T., & Maglott, D. R. (1971) *Methods Enzymol. 20C*, 449–456.

Stöffler, G., & Wittmann, H. G. (1977) *Mol. Mech. Protein Biosynth.*

Thomas, G. J., Jr. (1970) *Biochim. Biophys. Acta 213*, 417–423.

Thomas, G. J., Jr. (1976) *Appl. Spectrosc. 30*, 483–494.

Thomas, G. J., Jr., & Hartman, K. A. (1973) *Biochim. Biophys. Acta 312*, 311–322.

Thomas, G. J., Jr., & Kyogoku, Y. (1977) in *Infrared and Raman Spectroscopy, Practical Spectroscopy Series*, (Brame, E. G., Jr., & Grasselli, J. G., Eds.) Vol. 1 (Part C), pp 717–872, Marcel Dekker, New York.

Thomas, G. J., Jr., Medeiros, G. C., & Hartman, K. A. (1971) *Biochem. Biophys. Res. Commun. 44*, 587–592.

Thomas, G. J., Jr., Chen, M. C., & Hartman, K. A. (1973) *Biochim. Biophys. Acta 324*, 37–47.

Van Holde, K. E., & Hill, W. E. (1974) *Ribosomes* [*Meet.*].

Wool, I. G. (1979) *Annu. Rev. Biochem. 48*, 719–754.